The telescope assembly of the Ariel space mission: an updated overview

Emanuele Pace, Manuel Adler Abreu, Gustavo Alonso, Bruno Barroqueiro, Andrea Bocchieri, Daniele Brienza, Anna Brucalassi, Paolo Chioetto, Carlos Compostizo, Fausto Cortecchia, Fabio D'Anca, Ciro Del Vecchio, Emiliano Diolaiti, Paul Eccleston, Salma Fahmy, Jose Fernandes, Alejandro Fernandez Soler, Debora Ferruzzi, Mauro Focardi, Sara Freitas, Camille Galy, Laura Garcia Moreno, Andres Garcia Perez, Daniele Gottini, Elisa Guerriero, Jean-Philippe Halain, Marie-Laure Hellin, Delphine Jollet, Riccardo Lilli, Giuseppe Malaguti, Laura Martì, Alexandra Mazzoli, Giuseppina Micela, Gianluca Morgante, Luca Naponiello, Vladimiro Noce, Enzo Pascale, Javier Perez Alvarez, Raffaele Piazzolla, Paolo Picchi, Giampaolo Preti, Stephane Roose, Mario Salatti, Jean-Christophe Salvignol, Antonio Scippa, Christophe Serre, Luca Terenzi, Giovanna Tinetti, Elisabetta Tommasi Di Vignano, Andrea Tozzi, Bart Vandenbussche, Paola Zuppella

Published version information:

Citation: Emanuele Pace et al., The telescope assembly of the Ariel space mission: an updated overview, Proceedings Volume 13092, Space Telescopes and Instrumentation 2024: Optical, Infrared, and Millimeter Wave; 130921C (2024)

DOI: https://doi.org/10.1117/12.3018735

The telescope assembly of the Ariel space mission
An updated overview

Emanuele Pace[*a,d], Manuel Adler Abreu[r], Gustavo Alonso[o], Bruno Barroqueiro[q], Andrea Bocchieri[i], Daniele Brienza[k], Anna Brucalassi[d], Paolo Chioetto[h,b,c], Carlos Compostizo[s], Fausto Cortecchia[e], Fabio D'Anca[g], Ciro Del Vecchio[d], Emiliano Diolaiti[e], Paul Eccleston[f], Salma Fahmy[t], Jose Fernandes[q], Alejandro Fernandez Soler[o], Debora Ferruzzi[d], Mauro Focardi[d], Sara Freitas[q], Camille Galy[n], Laura Garcia Moreno[o], Andres Garcia Perez[o], Daniele Gottini[d], Elisa Guerriero[g], Jean-Philippe Halain[t], Marie-Laure Hellin[n], Delphine Jollet[t], Riccardo Lilli[m], Giuseppe Malaguti[e], Laura Martì[p], Alexandra Mazzoli[n], Giuseppina Micela[g], Gianluca Morgante[e], Luca Naponiello[u], Vladimiro Noce[d], Enzo Pascale[i], Javier Perez Alvarez[o], Raffaele Piazzolla[k], Paolo Picchi[d], Giampaolo Preti[a,d], Stephane Roose[n], Mario Salatti[k], Jean-Christophe Salvignol[t], Antonio Scippa[m], Christophe Serre[p], Luca Terenzi[e], Giovanna Tinetti[l], Elisabetta Tommasi Di Vigano[k], Andrea Tozzi[d], Bart Vandenbussche[j], Paola Zuppella[h,c]

[a]Dip. Fisica ed Astronomia, Università di Firenze, Largo E. Fermi 2, 50125 Firenze, Italy
[b]Centro di Ateneo di Studi e Attività Spaziali "Giuseppe Colombo", Via Venezia 15, 35131 Padova, Italy
[c]INAF-Osservatorio Astronomico di Padova, Vicolo dell'Osservatorio 5, 35122 Padova, Italy
[d]INAF-Osservatorio Astrofisico di Arcetri, Largo E. Fermi 5, 50125 Firenze, Italy
[e]INAF-Osservatorio di Astrofisica e Scienza dello Spazio di Bologna, Via Piero Gobetti 93/3, 40129 Bologna, Italy
[f]RAL Space, STFC Rutherford Appleton Laboratory, Didcot, Oxon, OX11 0QX, UK
[g]INAF-Osservatorio Astronomico di Palermo, Piazza del Parlamento 1, 90134 Palermo, Italy
[h]CNR-Istituto di Fotonica e Nanotecnologie di Padova, Via Trasea 7, 35131 Padova, Italy
[i]Dip. Fisica, La Sapienza Università di Roma, Piazzale Aldo Moro 2, 00185 Roma, Italy
[j]KU Leuven Instituut voor Sterrenkunde, Celestijnenlaan 200D bus 2401, 3001 Leuven, Belgium
[k]ASI, Agenzia Spaziale Italiana, Via del Politecnico snc, Roma, Italy
[l]Dept. Physics and Astronomy, University College London, Gower Street, London WC1E 6BT, UK
[m]Dip. Ingegneria Industriale, Università di Firenze, Via Santa Marta, 3 50139 Firenze, Italy
[n]Centre Spatial de Liège, Université de Liège, Avenue du Pré-Aily, B-4031 Angleur, Liège, Belgium
[o]Universidad Politécnica de Madrid, Plaza del Cardenal Cisneros 3, 28040 Madrid, Spain
[p]Institut d'Estudis Espacials de Catalunya, Gran Capità, 2-4, Edifici Nexus, Desp. 201 08034 Barcelona, Spain
[q]Active Space Technologies S.A., Parque Industrial de Taveiro, Lote 12, 3045-508 Coimbra, Portugal
[r]University of Lisbon, Institute of Astrophysics and Space Sciences, Campo Grande, Lisboa, Portugal
[s]Sener Aerospacial, Zugatzarte Etorb., 56, 48930 Getxo, Bizkaia, Spain
[t]ESA-ESTEC, Keplerlaan 1, 2201 AZ Noordwijk, The Netherlands
[u]INAF-Osservatorio Astrofisico di Pino Torinese, Via Osservatorio 20, Pino Torinese, Torino, Italy

Space Telescopes and Instrumentation 2024: Optical, Infrared, and Millimeter Wave,
edited by Laura E. Coyle, Shuji Matsuura, Marshall D. Perrin, Proc. of SPIE Vol.
13092, 130921C · © 2024 SPIE · 0277-786X · doi: 10.1117/12.3018735

ABSTRACT

Ariel (Atmospheric Remote-Sensing Infrared Exoplanet Large Survey) is the adopted M4 mission in the framework of the ESA "Cosmic Vision" program. Its purpose is to survey the atmospheres of known exoplanets through transit spectroscopy. The launch is scheduled for 2029. The scientific payload consists of an off-axis, unobscured Cassegrain telescope feeding a set of photometers and spectrometers in the waveband 0.5-7.8 μm and operating at cryogenic temperatures (55 K). The Telescope Assembly is based on an innovative fully aluminum design to tolerate thermal variations to avoid impacts on the optical performance; it consists of a primary parabolic mirror with an elliptical aperture of 1.1 m (major axis), followed by a hyperbolic secondary that is mounted on a refocusing system, a parabolic re-collimating tertiary and a flat folding mirror directing the output beam parallel to the optical bench. An innovative mounting system based on three flexure hinges supports the primary mirror on one of the optical bench sides. The instrument bay on the other side of the optical bench houses the Ariel IR Spectrometer (AIRS) and the Fine Guidance System / NIR Spectrometer (FGS/NIRSpec). The Telescope Assembly is in phase C towards the Critical Design Review; the fabrication of the structural and engineering models is in progress; some components, i.e., the primary mirror and the flexure hinges, are undergoing further qualification activities. This paper aims to update the scientific community on the progress concerning the development, manufacturing, and qualification activity of the ARIEL Telescope Assembly.

Keywords: space telescope, Ariel mission, Infrared Telescope, cryogenic telescope, Cassegrain, aluminum mirror

1. INTRODUCTION

The European Space Agency (ESA) adopted Ariel (Atmospheric Remote-sensing Infrared Exoplanet Large-survey) in November 2020 as the M4 mission under the ESA 2015-2025 Cosmic Vision Program. Ariel will address the fundamental questions on what exoplanets are made of and how planetary systems form and evolve, investigating the atmospheres of hundreds of diverse planets orbiting different types of stars. Ariel will observe a large number (~1000) of warm and hot transiting gas giants, Neptunes, and super-Earths around a range of host star types using differential spectroscopy in the ~ 1.1 – 7.8 μm spectral range and broad-band photometry in the optical and Near-IR. Generally, planets hotter than 600 K will be targeted to exploit their well-mixed atmospheres. Ariel is scheduled to launch in 2029.[1]

The Ariel Payload Module (PLM) consists of Cold Units based on an afocal, unobscured Cassegrain-type telescope[2] feeding a collimated beam through a Common Optics system into two separate instrument modules: the FGS[3], a combined Fine Guidance System/VIS-Photometer/NIR-Spectrometer and the Ariel Infra-Red Spectrometer (AIRS)[4], a 2-channel low-resolution IR spectrometer. The PLM is passively cooled to ~55 K; three V-Groove radiators shield it thermally from the warm service module (SVM). The SVM hosts the usual spacecraft subsystems like avionics or propulsion but also the warm units of the payload, namely the Instrument Control Unit (ICU), the Detector Control Unit (DCU), the Telescope Control Unit (TCU), and the FGS Control Unit (FCU) electronics.

2. THE TELESCOPE ASSEMBLY OVERVIEW

The Ariel Telescope Assembly (TA) is an all-aluminum, off-axis Cassegrain telescope operating at cryogenic temperature (~ 55 K). It feeds a collimated beam into two separate instrument modules in the Telescope Optical Bench (TOB) behind the Primary Mirror M1. The telescope metering structure (TMS) is fixed to the TOB on one side and supports the M2 mirror coupled to the M2 mechanism (M2M) on the other. The TA is supported by three couples of Bipods and shielded thermally by 3 V-Grooves (see Fig.1).

The main characteristics of the Ariel Telescope are detailed in Tab.1. Its optical system consists of four mirrors: M1 (elliptical with axes of 1.1 m x 0.7 m), M2, M3 (with a smaller diameter of the optical area at ~ 112 mm and 30 mm, respectively), and a 31 mm diameter flat folding mirror (M4). All the mirrors are made of high-grade aluminum to ensure excellent thermal stability. The considerable size of the primary mirror led to the implementation of a lightening process to reduce the mass. Additionally, the entrance baffle, an aluminum shield surrounding the M1 mirror, limits its field of view, while an additional baffle blocks any direct view of the sky from M2. M2 is mounted on a refocusing mechanism (M2M) with three freedom degrees (focus and tip/tilt) designed to correct movements after launch and subsequent cooling and potentially make occasional adjustments to compensate for long-term drifts in structural stability.

The refocusing mechanism has a heritage developed in previous ESA studies and programs: similar mechanisms have been provided for the Gaia and Euclid telescopes[5,6].

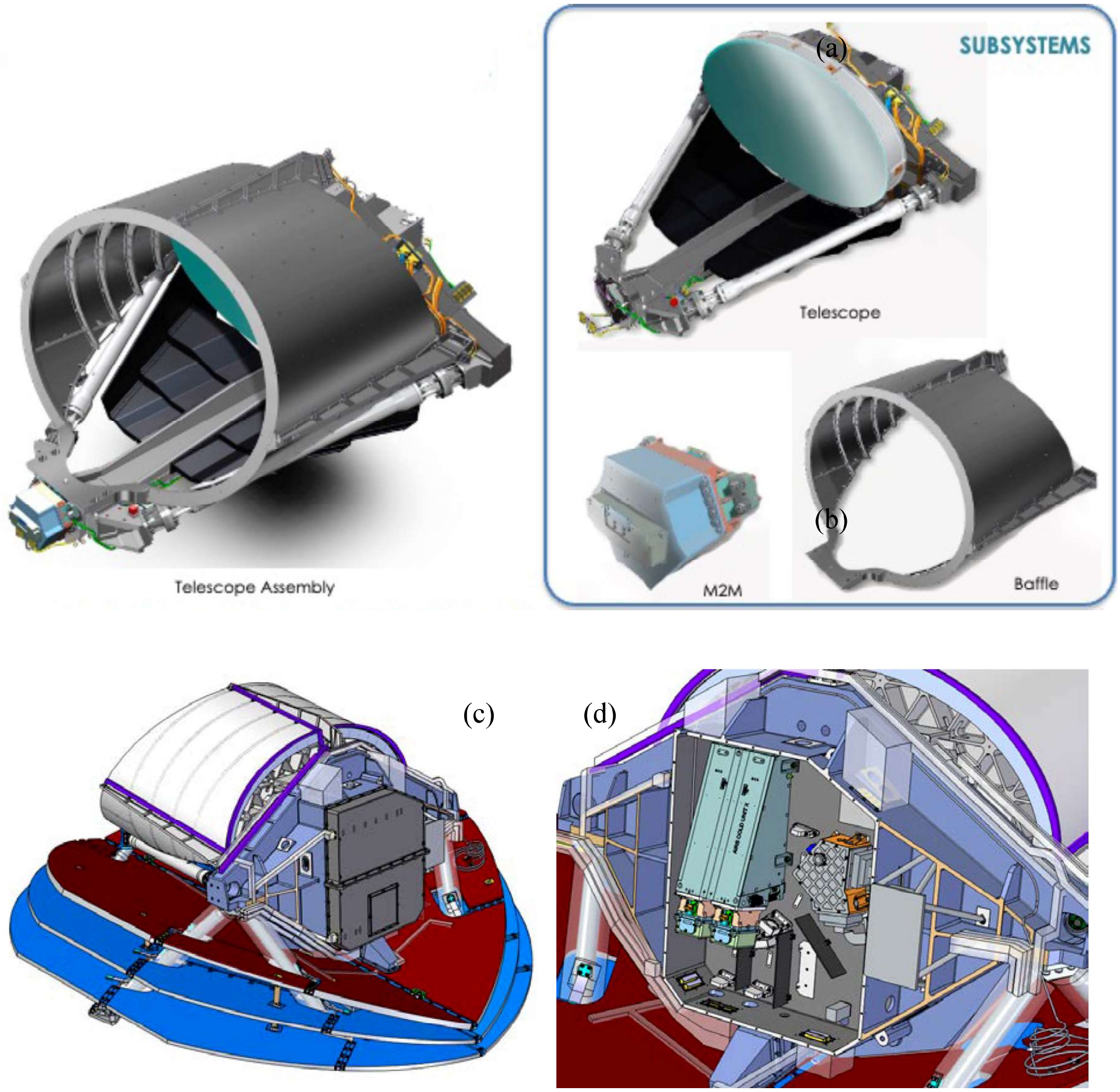

Figure 1. (a) Telescope assembly and bipods; (b) front view of the M1 mirror; (c); the Ariel payload showing the back of the telescope closed by the instrument radiator and the V-Grooves; (d) the optical bench and the instrument cavity.

The M1 mirror is supported directly by the optical bench on one side, while the two main instruments and the Common Optics are located on the other side. M2 and M3 mirrors are thermally decoupled from the support structures to improve the telescope stability; M2 is mounted on the M2 refocusing mechanism. To enhance the structural stiffness of the telescope, the optical bench is provided in a position close to the midpoint of its major axis, with two aluminum alloy bars that connect OB directly to the M2 structure. The baffle is connected to the optical bench both thermally and mechanically, which contributes significantly to the thermal stability of the telescope. This thermomechanical design ensures the required stiffness and excellent thermal conductivity in all directions. Therefore, M4 serves as the optical interface of the TA to the Common Optics. Mechanical interfaces are located at the bipods, the instrument radiator, the FGS and AIRS instruments, and the supports of the Common Optics.

Table 1. Main characteristics of the Ariel Telescope

Parameter	Value
Entrance pupil size	1100 x 730 mm
FoV	30" with diffraction limited performance 41" with optical quality TBD allowing FGS centroiding 50" unvignetted
Wavelength range	0.5 – 8 μm
WFE	Diffraction limited ≤ 3 μm (200 nm RMS)
M1 WFE	≤ 160 nm RMS
M1 roughness	< 10 nm RMS
M2, M3, M4 roughness	< 2 nm RMS
Exit pupil (beam size)	20.4 x 13.3 mm

3. THE OPTICAL DESIGN

The Ariel TA is an off-axis Cassegrain telescope (M1 parabola, M2 hyperbola) followed by a re-collimating off-axis parabola (M3), a plane fold mirror (M4), and the exit pupil plane. M1 shares with M2 and M3 a common optical axis, which lies parallel to the ARIEL X axis. Fig.2 shows the optical layout of the Ariel Telescope, while Tab.2 and Tab.3 summarize the main optical parameters of the TA mirrors.

Table 2. Main optical parameter values of the Telescope Assembly mirrors (* @ 50K)

Optical element	M1	M2	M3	M4
Type	Concave mirror	Convex mirror	Concave mirror	Plane mirror
Clear aperture shape	Elliptical	Elliptical	Elliptical	Circular
Clear aperture size (mm)*	1100 x 747.81	110 x 80	28 x 20	24
Mirror dimensions (mm)*	1125 x 771	130 x 100	50 x 45	50
R (mm)*	2319.393	239.137	511.771	Infinite
k	-1	-1.392	-1	0
Off-axis value (mm)	502	50	20	0
Surface roughness (nm RMS)	10	2	2	2
Mirror material	aluminum	aluminum	aluminum	aluminum
IR Reflective coating	Silver	Silver	Silver	Silver

[1] The collecting area is 1100 x 730 mm @ 50K due to the M1 inclination angle of 12.165°.

The direction of the telescope optical axis (defined by the M1, M2, and M3 optical common axis) is parallel to the X_{ARIEL} axis. The telescope pointing axis, or line of sight (LOS), is offset by 0.1° to the optical axis to give an accessible return beam from M3.

The optical coordinate system is defined as follows:

- The origin is located at the vertex of the parent parabola for M1.
- Z_{OPT} is parallel to the telescope's optical axis (defined by the M1, M2, and M3 optical common axis) and is positive in the direction of the incoming light. Z_{OPT} is parallel to X_{ARIEL}.
- Y_{OPT} is perpendicular to Z_{OPT} and the separation plane between the LV adaptor and the s/c. It is positive in the direction from the separation plane towards the payload. Y_{OPT} is parallel to Z_{ARIEL}.
- X_{OPT} completes a right-handed set.

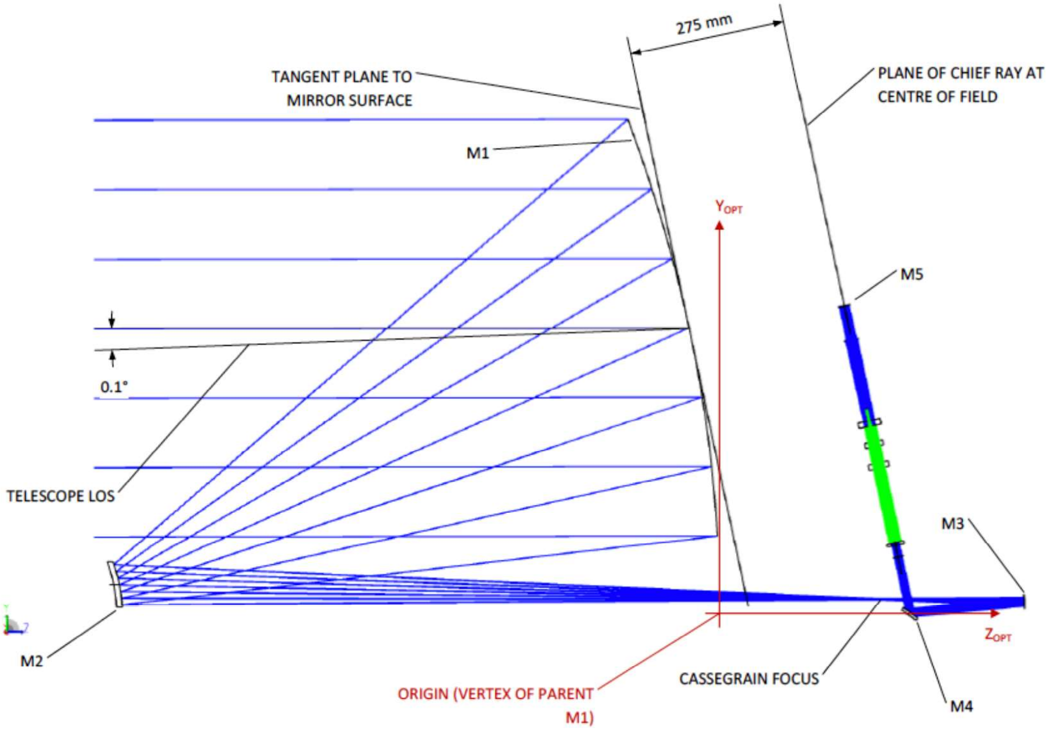

Figure 2. Scale drawing of the Ariel telescope – view in Y_{OPT}-Z_{OPT} plane. The 0.1° offset is exaggerated for clarity.

The 0.1° offset between Z_{OPT} and the telescope LOS is a rotation about X_{OPT}, in the direction shown in the system aperture stop at the M1 surface.

M4 is positioned to direct the beam onto the telescope optical bench such that all subsequent beams at the center of the field lie in a plane parallel to the tangent plane to the mirror surface. The chief ray at the center of the field is 275 mm from the tangent plane to the mirror surface. The beam on the optical bench has its major axis parallel to the plane of the optical bench. The beam size on the optical bench is 20 mm x 13.3 mm @ operational temperature 50 K.

The telescope exit pupil aperture is reported in Tab.3; the pupil's major axis is parallel to the plane of the optical bench. Given the optical magnification of 55 (spectral) and 54.7 (spatial), it translates to an entrance pupil at the M1 surface (system Stop) with size 1100 mm × 730 mm @ operational temperature 50K.

The design includes three configurations corresponding to the FGS and the two IR spectrometer channels. No refractive elements with any power are used, so it is sufficient to trace a single wavelength (3 µm is chosen).

4. THE MECHANICAL DESIGN

4.1 Overview

The main components of the TA relevant to the mechanical design are:

- Telescope Optical Bench
- Telescope Metering Structure
- Primary mirror M1 with its mounting system
- Secondary mirror M2 supported by an M2 refocusing mechanism (M2M)
- M3, M4 mirrors
- Baffle system

All the structural elements and the telescope mirrors are made of very high-grade aluminum to provide scalable mechanical properties at the different temperatures experienced by the telescope. To increase the rigidity of the structure, the optical bench and the bipod legs have been optimized in position, angle, and thickness, including the instrument box in the optical bench, and adding stiffening ribs has enhanced the global stiffness.

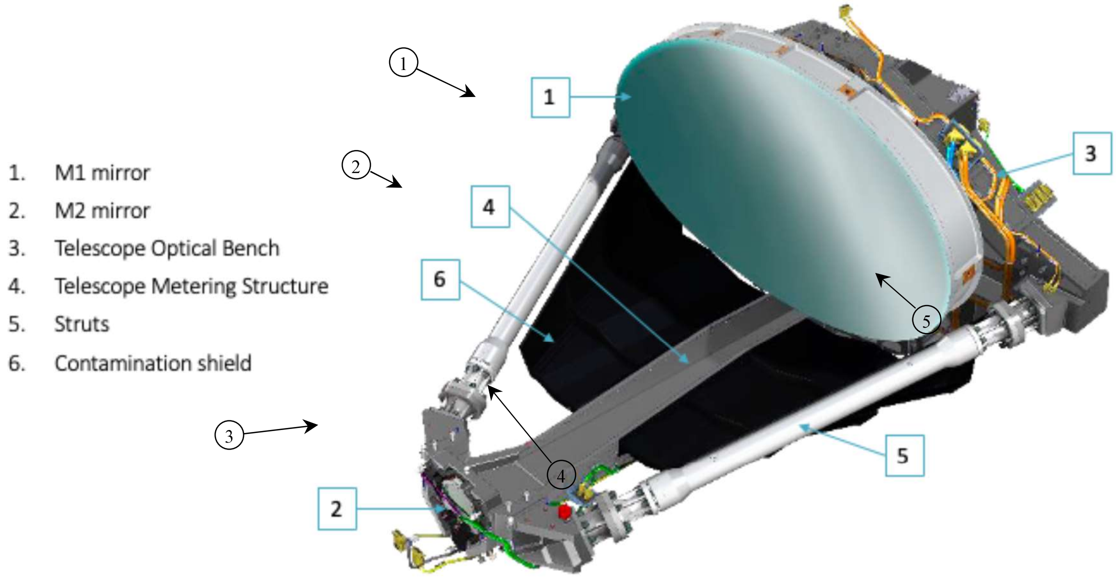

Figure 3. Mechanical assembly of the Ariel Telescope

The structure has been reinforced by the insertion of lateral struts, as Fig.3 shows. These arms ensure minimal deformations and high bending stiffness between M1 and M2 under in-plane and out-of-plane loads. The baffle surface is mechanically and thermally connected to the TOB. This thermo-mechanical design can guarantee at the same time rigidity and high thermal conductance.

The main components of the TA are hereafter discussed. However, work is in progress during phase B2 to improve the design of M1 and its mounting, the TOB thermo-mechanical coupling with M1 and baffle B1, the B1 baffle and the overall mechanical design to improve matching with the TA and Payload requirements.

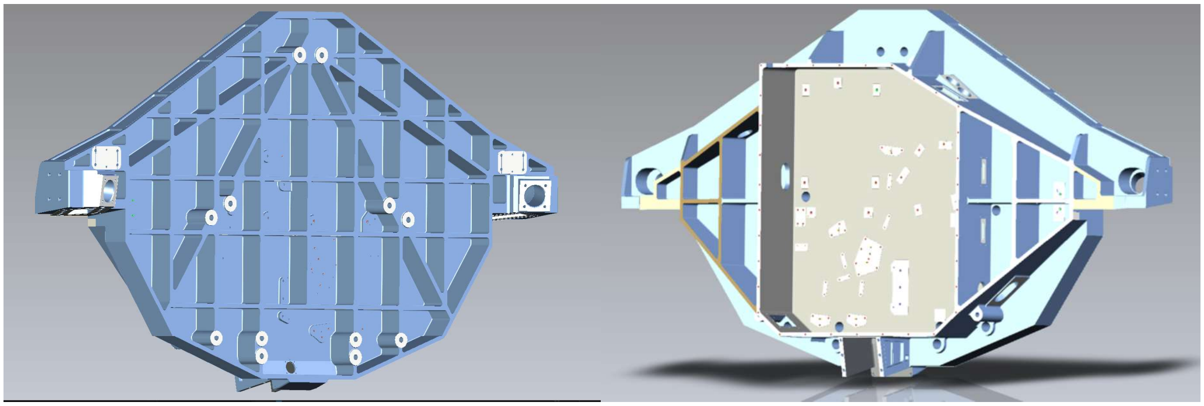

Figure 4. The Telescope Optical Bench. The mechanical, optical, and electrical interfaces are clearly shown.

4.2 Telescope Optical Bench and Metering Structure

A mass saving and optimization activity on the optical bench and the metering structure has been performed. This has cleaned up most of the features that evolved during the project development. In addition, the number of stiffeners on the front surface has been significantly reduced. The thickness of the central plane and stiffening ribs have also been revised to minimize mass. The design is still evolving in detail. The unit shown in Fig. 4 is the TOB.

This component is crucial for the whole Ariel Payload. It has critical interfaces on both surfaces. The instrument cavity (Fig. 4, right panel) must provide a stable mechanical and thermal environment for the instruments. On the front surface, it serves as the critical interface to the M1 mounting system through six fixing bolts (in the upper part of the left panel in Fig. 4; the lower bolts are for fixing the TMS).

All components are manufactured from the same grade of aluminum to ensure uniform thermo-mechanical behavior of the whole assembly. This is a crucial issue in the telescope design and has been thoroughly addressed in the STOP analysis. The TOB is directly supported on the two large rear bipods (not part of the TA), which utilize titanium flexures.

Currently, the telescope optical bench is manufactured using conventional machining techniques using a single piece of aluminum. This is to ensure that there are no thermal discontinuities of joints and to minimize manufacturing risk. The optical bench thickness has been increased to include the instrument box as part of the structure using stiffening ribs on the front and rear surfaces. This H section gives the bench a high structural rigidity to out-of-plane load (high mass of objects). The beam that runs from the TOB to the M2M position is the TMS. Two lateral struts connect the TMS front edge to the TOB to improve the mechanical rigidity.

4.3 M1 mounting system

The M1 mounting based on flexure hinges is rigid to the TOB (see Fig. 5). This innovative mounting provides a planarity compensation through a conical-spherical joint and the required level of isostatic mounting to minimize distortions induced in the mirror. The mounting minimizes mechanical stresses on the mirror, ensuring sufficient rigidity and strength to withstand the launch environment. The hinges' design was selected after a detailed comparative study. This investigated different solutions, such as the whiffle-tree design, standard hexapods, blade flexures, and flexure hinges, to solve mechanical and thermal constraints like minimal volume for any mounting system and mass budget. The mounting design based on flexures looks promising, even if a huge design effort addressed the TOB-to-flexure and mirror-to-flexure interfaces to minimize any deformations that the mechanical coupling induced on the optical surface.

A prototype of the flexure hinges was manufactured to test the manufacturability of this mounting system. It is currently tested coupled to the M1 structural model to assess the validity of this innovative solution.

4.4 Mirrors

The primary and secondary mirrors M1 and M2 are arranged in an off-axis Cassegrain configuration with the TOB supporting M1 and M2 at the end of the TMS, as shown in Fig. 3.

Furthermore, M2 and M3 are thermally isolated from the supporting structures to ensure their thermal stability. The M2 is mounted on the TMS, an aluminum arm rigidly connected to the TOB and equipped with a refocusing mechanism (M2M) at the other end. The central bipod of the Ariel PLM supports the TMS and the M2M. M3 and M4 are positioned at the end of the TMS and beneath the TOB.

The mirrors will be manufactured from the same very high-grade aluminum substrate, and each will have a protected silver coating on the optical surface to improve the reflectivity in the Ariel spectral range. M1 will be lightened by > 30% to reduce the mass. The lightweight level has been designed as the best trade-off between reducing the mass and keeping the optical surface quality in the SFE requirements.

5. THE THERMAL DESIGN

5.1 Overview

The thermal design of the spacecraft is based on a cold Payload Module sitting on the top of a warm Service Module The upper surface of the Service Module has an estimated average operational temperature ranging between 253 K (hereafter defined as Cold Case) and 293K (hereafter defined as Hot Case). The TA, enclosed in the cold environment established by the last V-Groove, acts as an extra passive stage using its large Baffle and Optical Bench as radiating surfaces. These radiators coated with high-IR emissivity paint improve the efficiency and performance of the entire PLM's passive cooling system. The whole telescope structure and the mirrors reach temperatures around 55 K at a steady state in the Hot Case. Six primary thermal interfaces exist between the TA and the rest of the payload (excluding the units on the TOB):

- Four conductive interfaces with the head of the bipods. These four interfaces are expected to operate in the 58 – 63 K range and, in the Hot Case, can inject into the TA a heat leak of 36 mW per rear bipod and 69 mW for each front bipod.
- The cryo-harness injects an extra conductive leak. Currently, this heat flux is less than 150 mW in the Hot Case due to the parasitic interception of the V-Grooves.
- The last V-Groove (VG3, around 62 K in the Hot Case) and the deep space (3 K) determine the radiative environment. The irradiated total heat leak from VG3 to the TA is about 180 mW in the Hot Case.

The primary mirror (M1) mounting system is designed to achieve the optimal level of thermal coupling to the Optical Bench. On one side, the flexures must ensure a certain level of insulation to dampen any temperature fluctuation that could be transmitted to the mirror from the rest of the payload. At the same time, they must guarantee a conductance high enough to limit the thermal gradient between the mirror and the bench during cool-down/warmup to avoid any thermally generated mechanical stress.

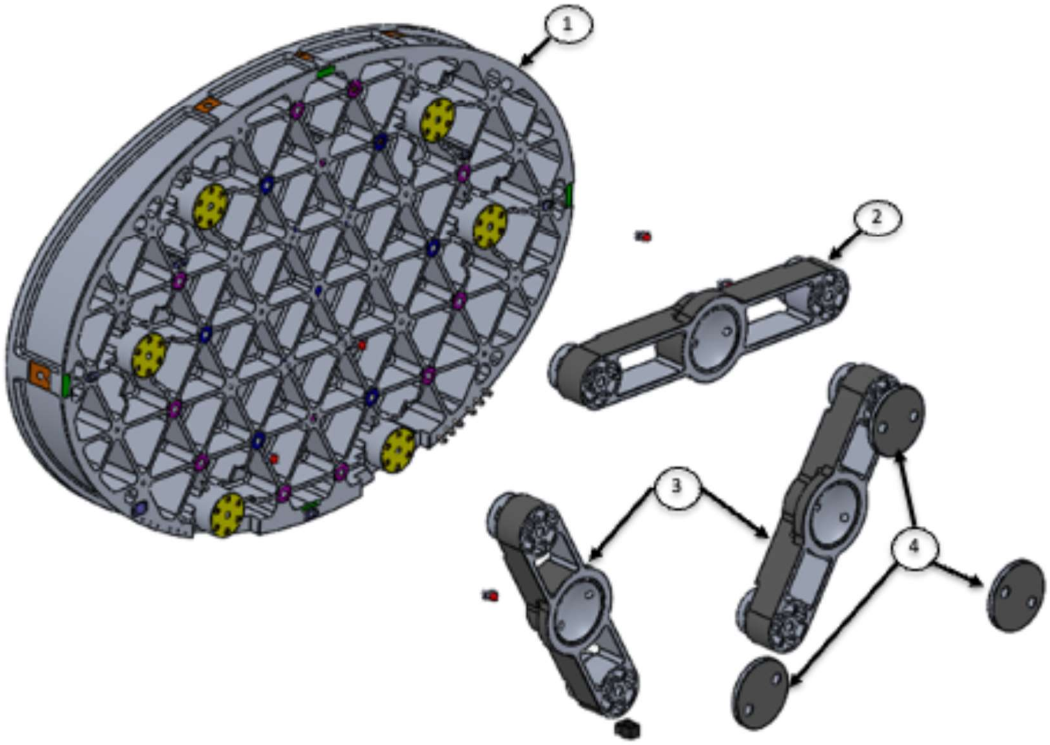

Figure 5. (1) M1 mirror; (2 & 3) flexure hinges and (4) hemispherical pads interfacing the flexures with the TOB.

5.2 Telescope Assembly GTMM

The TA is the largest component of the PLM Geometrical and Thermal Mathematical Model (GTMM). The TA average temperature is around 52.5 K and 55 K in the Cold and Hot Cases, respectively. The 3 K difference between the two extreme cases, when the PLM interface temperature differs by nearly 40 K, shows a very high level of insulation from the warm part of the S/C reached with the present PLM/TA thermal architecture.

In the two thermal cases, M1 operates around 53.5 K and 55.5 K with a total gradient across its surface of less than 5 mK due to the good thermal uniformity of the mounting interfaces on the TOB and the good thermal conductance of the mirror itself. The thermal stability of the mirrors is another relevant factor concerning the TA performance. The spacecraft interface is designed to withstand thermal instability of up to 10 K over 10 hours.

The worst-case fluctuations are the slowest ones, as they are not filtered out efficiently by the thermal capacitance of the PLM. For this reason, to simulate the effect of this fluctuation level on the mirrors, a slow but constant decreasing rate of 1K/h over 10 hours is assumed at the SVM interface temperature, and the impact on M1 and M2 is analyzed. The two mirrors show a different behavior with time. The temperature of the M1 remains almost constant, decreasing by a small fraction of a mK due to the excellent thermal insulation and the high thermal capacitance of the primary mirror. The M2, on the other side, is less insulated from the Telescope Metering Structure, has a lower capacitance, and can feel the influence of the shorter, thus more conductive, front bipod. For these reasons, its temperature change is of the order of 2 mK. In summary, the TA thermal design shows a very high level of insulation and stability for both mirrors. There are still margins to increase the thermal resistance of the M2 from the TMS, if necessary, to minimize any impacts of potential conducted fluctuations further.

5.3 Thermal Control System

The TA thermal performance is based on a purely passive architecture, part of the general PLM Thermal Control System. The thermal status of the TA is continuously monitored by a set of thermistors controlled by the TCU. The task of this monitoring system is to measure the temperature of some thermal reference points and critical units, as mirrors M2M and TOB, to check their thermal status and health. At present, no need for active thermal control of M1 is expected. However, it is agreed to keep open in the TCU design the option of having active control of M1 if the need for temperature stabilization of M1 arises because of the results of the STOP analysis. The TA thermal monitoring system is combined with a separate set of thermistors and heaters needed for Decontamination and Survival heating to avoid condensation of contaminants during the cool-down phases.

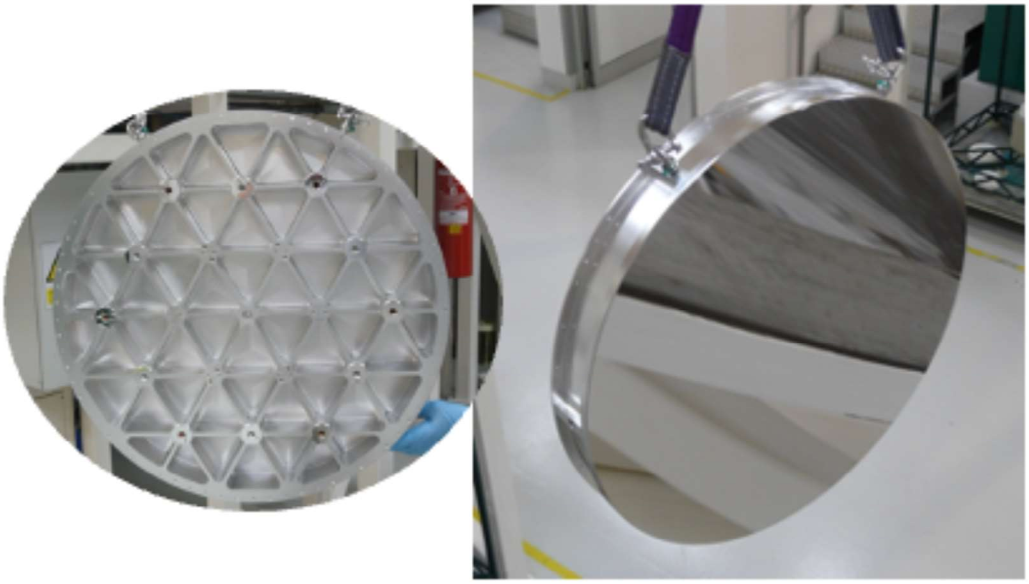

Figure 6. The M1 breadboard BB#1

6. TECHNOLOGY DEVELOPMENT ACTIVITIES

Some technology development activities (TDA) were running during the project phases A and B. The aim was to face and solve the technology risks related to the aluminum mirrors and the M2 refocusing mechanism (M2M). The mirror M1 still has some technical issues that require a prolonged development phase. Following a TDA program addressing de-risking of the manufacturing processes, the thermal stability of the large-size aluminum mirror operating at cryogenic temperature, and the protected silver coating, the TRL of the Al M1 mirror has been raised to 6 at the TA PDR. However, this activity concluded that part of the polishing process needs further investigation to reduce the "orange-peel" effect that introduces medium-low frequencies in the mirror surface front error; hence, ongoing activities are still being conducted on two identical breadboards.

The two M1 breadboards will follow different development tasks:

- BB#1 was produced following the same manufacturing steps as Ariel M1 and is currently undergoing an additional polishing step, which shows promise in removing the medium-low frequencies (see Fig. 6).
- BB#2 was produced to de-risk the manufacturing processes, i.e., roughing, lightening, diamond turning, and polishing. A nickel-phosphorus (NiP) coating will be applied to create a significantly harder surface, improving the optical quality of the mirror surface. The differential CTE at the operational temperature is a concern; it will be tested at the cryogenic facility at INAF-OAS, Italy.

Some encouraging results have already been achieved:

1. The infrared high-reflectivity protected silver coating has been qualified and can withstand the warm-cryogenic thermal cycles.
2. The diamond-turning process provides specifications better than the requirements on the breadboard mirrors.
3. The thermal cycling recipe provides a better material in terms of size and distribution of agglomerates and internal stresses; the results on the PTM suggest that the mirror is stable after all the thermal treatments.

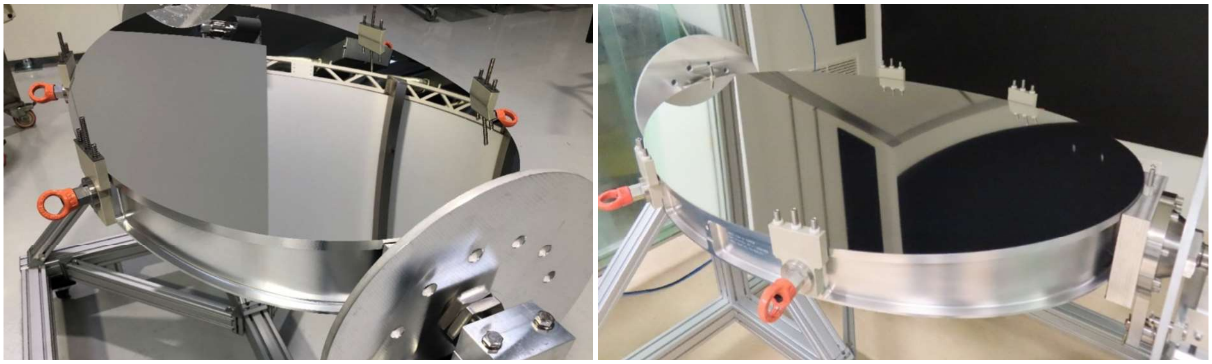

Figure 7. The M1 mirror models: M1 SM on the left and M1 EM on the right.

7. OVERVIEW OF THE MANUFACTURING

The M1 Structural Model (SM) and Engineering Model (EM) have been manufactured and are ready for testing and integration (see Fig. 7). In particular, the M1 SM has been used for the commissioning of the new diamond turning machine that LT Ultra Precision developed for machining mirrors as large as 1.2 meters. Being the diamond-turned mirror surface measurable interferometrically, the M1 SM is currently undergoing comprehensive optical-mechanical tests at INAF Arcetri, Italy. The aim is to assess the M1-to-flexure interface by measuring the deformations that the mechanical coupling introduces. Another task of the current test is to check a new mirror support, allowing the subtraction of the gravity effects on the optical surface to put in evidence the actual optical aberrations.

The M1 EM mirror is polished at Media Lario and silver-coated at Cilas by using a variable-speed process to optimize the coating uniformity. The shape error is within the spec (60 nm rms), while the roughness is below the 10 nm rms spec (5.2 nm rms). In terms of cosmetics, the affected area is estimated at 0.11% and the "orange peel" effect is comparable to what has been measured for BB#1, thus requiring further polishing development as mentioned above.

M2, M3, and M4 EM mirrors have been diamond-turned and NiP-coated and they are undergoing polishing. The Structural model of these mirrors is a dummy mass included in the M2m and the TMS.

The TOB, TMS, and the other mechanical parts of the SM and EM are manufactured in parallel and they should be available soon for the telescope integration activity. The plan is to deliver the telescope models for PLM test campaigns by the end of 2024 and mid-2025.

ACKNOWLEDGMENTS

The TA Scientific Team acknowledges the industrial partners, Leonardo S.p.A. and Media Lario s.r.l. for their support in the design and manufacturing of the telescope parts. This activity has been developed under the Implementation Agreement n. 2021-5-HH.0 “Italian Participation to Ariel mission phase B2/C” between the Italian Space Agency (ASI) and the National Institute for Astrophysics (INAF) and under the ASI contracts n. 2021-21-I.0 “ARIEL TA Phase B Industrial Activities” and n. 2023-42-I.0 "ARIEL TA Phase C/D1 Industrial Activities".

REFERENCES

[1] Tinetti, G., et al., “A chemical survey of exoplanets with ARIEL”, Experimental Astronomy 46, 135–209 (Nov. 2018).
[2] Da Deppo, V., Middleton, K., Focardi, M., Morgante, G., Claudi, R., Pace, E., and Micela, G., “The optical configuration of the telescope for the ARIEL ESA mission,” Proc. SPIE 10698, 106984O (2018).
[3] Rataj, M., Wawer, P., Skup, K., Sobiecki, M., "Design of fine guidance system (FGS) for ARIEL mission," Proc. SPIE 11176, 111763E (2019).
[4] Amiaux, J., Berthé, M., Boulade, O., Cara, C., Lagage, P.O., Moreau, V., Hamm, V., Morinaud, G., Ollivier, M., André, Y., Geoffray, H., Eccleston, P., Middelton, K., Pascale, E., Frericks, M., Focardi, M., Pace, E., EPSC2018-652-1, 12 (2018).
[5] Ramos Zapata, G., Sánchez Rodríguez, A., Belenguer Dávila, T., Urgoiti E., Ramírez Quintana, A., "Optical tests of a space mechanism under an adverse environment: GAIA secondary mirror mechanism under vacuum and thermally controlled conditions," Proc. SPIE 6671, 667117 (2007).
[6] Artiagoitia, A., Compostizo, C., Rivera, L., Proc. ‘ESMATS 2017’ (2017).
[7] https://www.thorlabs.com/
[8] Raymond G. Ohl IV, Michael P. Barthelmy, Said Wahid Zewari, Ronald W. Toland, Joseph C. McMann, David F. Puckett, John G. Hagopian, Jason E. Hylan, John Eric Mentzell, Ronald G. Mink, Leroy M. Sparr, Matthew A. Greenhouse, John W. MacKenty, "Comparison of stress-relief procedures for cryogenic aluminum mirrors," Proc. SPIE 4822 (2002).